

Radiographic texture of the trabecular bone of the proximal phalanx in horses with metacarpophalangeal osteoarthritis

Lorena de Oliveira PEREIRA^{1*}, Anderson Fernando DE SOUZA¹, Julio David SPAGNOLO¹, Ana Lúcia Miluzzi YAMADA¹, Daniela Miranda Richarte de Andrade SALGADO² and André Luis do Valle DE ZOPPA¹

¹School of Veterinary Medicine and Animal Science, University of São Paulo, São Paulo 05508270, Brazil

²School of Dentistry, University of São Paulo, São Paulo 05508000, Brazil

Osteoarthritis (OA) is a prevalent condition in horses, leading to changes in trabecular bone structure and radiographic texture. Although fractal dimension (FD) and lacunarity have been applied to quantify these changes in humans, their application in horses remains nascent. This study evaluated the use of FD, bone area fraction (BA/TA), and lacunarity in quantifying trabecular bone differences in the proximal phalanx (P1) in 50 radiographic examinations of equine metacarpophalangeal joints with varying OA degrees. In the dorsopalmar view, regions of interest were defined in the trabecular bone of the proximal epiphysis, medial and lateral to the sagittal groove of P1. Lower BA/TA values were observed medially in horses with severe OA ($P=0.003$). No significant differences in FD and lacunarity were found across OA degrees ($P>0.1$). FD, BA/TA, and lacunarity were not effective in identifying radiographic texture changes in the P1 trabecular bone in horses with different metacarpophalangeal OA degrees.

Key words: fractal analysis, horses, osteoarthritis, trabecular bone

J. Equine Sci.
Vol. 35, No. 2
pp. 21–28, 2024

Trabecular bone, noted for its fractal attributes, exhibits greater metabolic activity and a substantially higher renewal rate compared with compact bone, rendering it a superior marker for bone metabolic processes and an efficient tool for monitoring structural modifications. This capability is crucial for providing invaluable diagnostic insights [25]. Accordingly, the analysis of trabecular bone structure using fractal dimension (FD), bone area fraction (BA/TA), and lacunarity has been a focal point in several studies within human medicine and dentistry fields [16, 18, 19, 25, 26, 32, 34].

FD serves as a potent image texture descriptor, quantifying object complexity, with elevated values signifying more complex structures [7, 12, 19, 22, 37, 41]. However, given that distinct fractal objects may exhibit identical FDs, lacunarity is employed to augment FD, offering insights

into image heterogeneity [8, 15, 38] by evaluating the spatial arrangement of voids, hence elucidating the pixel distribution and organization, essentially quantifying space occupancy [3, 15]. Homogeneous objects display low lacunarity with consistent gap sizes, whereas heterogeneous entities demonstrate high lacunarity [43]. Additionally, the bone area fraction (BA/TA) is pivotal in determining the mechanical characteristics of trabecular bone and is associated with its mineral density, strength, and elasticity [14, 30, 39].

The use of FD, BA/TA, and lacunarity in analyzing trabecular bone has proven that there is a correlation with the mechanical properties of trabecular bone and is regarded as apt for delineating structural changes in bone in humans and others species, assisting in evaluating bone quality, repair mechanisms, functional adaptation, and conditions like osteoporosis and osteoarthritis (OA) [5, 13, 14, 16, 24, 30, 35, 44]. Several fractal analysis approaches have been documented, with the ImageJ software frequently utilized for analyzing images obtained via radiography, computed tomography, or bone histomorphometry to derive pertinent bone tissue parameters [17, 27]. Osteoarthritis, particularly prevalent in the metacarpophalangeal joint of horses, especially racers, instigates trabecular bone architectural

Received: January 19, 2024

Accepted: May 16, 2024

*Corresponding author. e-mail: lorenaoliveira@usp.br

©2024 Japanese Society of Equine Science

This is an open-access article distributed under the terms of the Creative Commons Attribution Non-Commercial No Derivatives (by-nc-nd) License. (CC-BY-NC-ND 4.0: <https://creativecommons.org/licenses/by-nc-nd/4.0/>)

alterations through bone remodeling, driven by osteoclasts and osteoblasts, under biochemical and mechanical influences [9, 19, 23].

Radiographic assessments provide a swift modality for bone tissue evaluation, with digital images portraying two-dimensional projections of intricate trabecular structures commonly adopted in fractal analyses [5, 19, 27, 43]. Jolley *et al.* (2006) illustrated the relative insensitivity of FD to variations in radiographic angles, densities, or machine settings, suggesting that its application to nonstandard radiographs is a potential area of research and potentially has diagnostic utility [25]. Despite its potential, the integration of fractal analysis into equine bone tissue research remains limited. This study aimed to evaluate the application of FD, BA/TA, and lacunarity in discerning radiographic differences in the proximal phalanx trabecular bone of horses with different degrees of metacarpophalangeal OA. We hypothesize that horses with less severe OA exhibit higher FD and BA/TA values and lower lacunarity, which are indicative of a denser, more intricate, and evenly distributed trabecular bone, compared with those with more advanced OA stages.

Materials and Methods

Data collection

The study received approval from the Ethics Committee for the Use of Animals at the School of Veterinary Medicine and Animal Science of the University of São Paulo, protocol number CEUAX No. 6884180522. We conducted a review of metacarpophalangeal joint radiographs of horses from the archive at the Service of Large Animal Surgery of the Veterinary Teaching Hospital of the School of Veterinary Medicine and Animal Science of the University of São Paulo. Fifty radiographic examinations from 50 distinct horses were chosen based on specific inclusion criteria: (i) horses aged three years or older; (ii) any sex, breed, or use for any sporting activity, excluding mules and donkeys; (iii) radiographic examinations included, at minimum, the lateromedial, dorsolateral-palmaromedial, dorsopalmar, and dorsomedial-palmarolateral views; (iv) horses without fractures, luxations, or deformities; and (v) radiographs free from movement or other artifacts that could compromise an accurate assessment of the images.

Classification of osteoarthritis

The selected radiographic examinations underwent analysis to determine the presence and severity of osteoarthritis. This assessment categorized the condition into the following four grades according to the criteria established by Silva *et al.* (2019) and Lacitignola *et al.* (2020) [29, 40], as outlined in Table 1: absent, mild, moderate, or severe

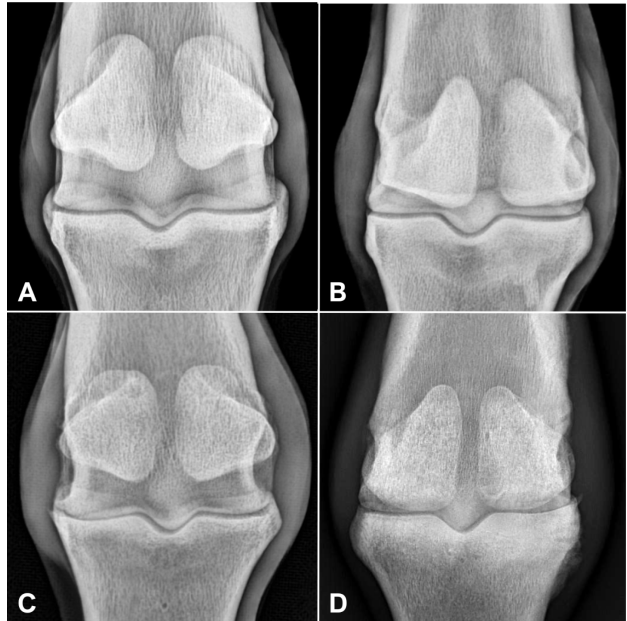


Fig. 1. Dorsopalmar radiographs of the metacarpophalangeal joint of horses showing the different grades of osteoarthritis (OA). (A) Absent, (B) Mild, (C) Moderate, (D) Severe.

(Fig. 1). Three independent evaluators, each with significant experience, conducted these assessments.

Definition of regions of interest (ROIs)

The dorsopalmar view enabled the identification of regions of interest (ROIs) measuring 50×50 pixels within the proximal epiphysis of the proximal phalanx. These ROIs were manually delineated on the trabecular bone, below the subchondral region and on both sides of the sagittal groove. To ensure consistency, ROIs were placed 30 pixels away from the joint line and centered along a line extending from the sagittal groove to the medial or lateral extremity. Subsequently, these ROIs were extracted, converted to 8-bit grayscale, duplicated, and then binarized (Fig. 2).

Fractal dimension, bone area fraction, and lacunarity

FD was determined using the box-counting method, while BA/TA was measured with the BoneJ plugin within the Fiji image processing package, a variant of the ImageJ software from the National Institutes of Health (Bethesda, MA, USA) [17]. Lacunarity was also assessed using the box-counting method, but through the FracLac extension. A single observer, who had undergone prior training, conducted all these measurements to ensure consistency and accuracy in the data collection process.

Table 1. Osteoarthritis severity classification for the metacarpophalangeal joint and corresponding radiographic findings

Degree	Severity	Radiographic findings
0	Absent	Normal radiographic aspect
1	Mild	Mild subchondral bone densification or focal areas of sclerosis Small osteophytes Mild joint space narrowing, with either symmetrical or asymmetrical presentation Slight calcifications in the tissues around the joint capsule or ligament attachment sites Subchondral bone margins with mild irregularity or superficial, localized erosions Single subtle osteochondral fragment without displacement Mild soft tissue hypertrophy Areas of localized soft tissue induration
2	Moderate	Moderate, diffuse subchondral sclerosis Prominent, organized osteophytes Moderate joint space narrowing, with either symmetrical or asymmetrical presentation, and preserved joint margins Well-defined and clearly visible enthesophyte Superficial and generalized subchondral erosions Well-defined, non-displaced osteochondral fragment Moderate soft tissue hypertrophy Areas of widespread soft tissue induration
3	Severe	Evident and diffuse subchondral sclerosis extending to the epiphyseal trabecular bone Extensive and irregular osteophytes Severe joint space narrowing with poorly defined or complete loss of joint margins Evident irregular, and disorganized enthesophytosis Severe subchondral erosion or cystic lesion Multiple non-displaced osteochondral fragments or a single displaced fragment Severe soft tissue hypertrophy Diffuse and generalized soft tissue induration

Adapted from Silva *et al.* (2019) and Lacitignola *et al.* (2020).

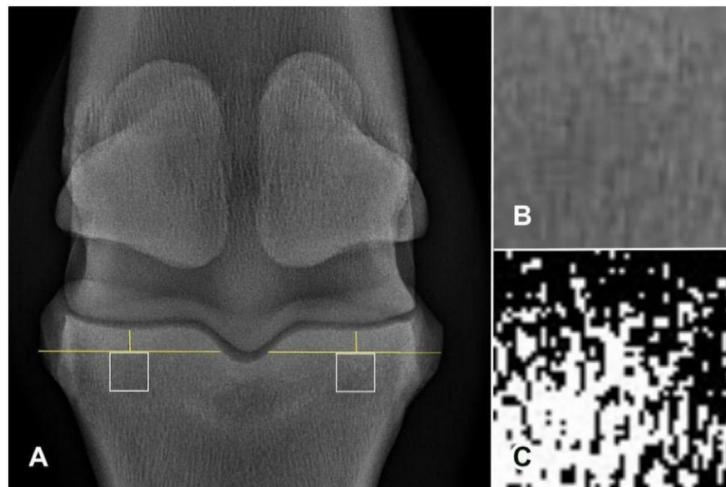


Fig. 2. (A) Dorsopalmar radiographic image of the metacarpophalangeal joint demonstrating the locations of the regions of interest (ROIs), (B) Duplicate ROI, (C) Binarized ROI.

Statistical analysis

Statistical analyses were conducted using the Jamovi software (version 2.3.21) [42]. To assess the consistency among evaluators in grading OA, the Kappa statistic was

employed. Descriptive statistics, including mean, median, standard deviation, minimum and maximum values, and 95% confidence intervals, were used to characterize the variables. Box plots illustrated the data distribution across

different OA degrees.

To evaluate the distribution of data, the Shapiro-Wilk test was applied for normality of residuals, and the Levene test was used to check the homogeneity of variance. Additionally, Q-Q plots were examined to further assess data normality. A generalized linear model, as part of the GAMLj package in Jamovi, was utilized for initial data analysis [21]. Factors like the degree of OA, sex, breed, age group, and their interactions were considered in the model. Model fit was verified using the likelihood ratio (log-likelihood) and the Akaike information criterion [1].

In the model, only the degree of OA emerged as a significant predictor ($P=0.003$). To compare the means across different OA degrees, an analysis of variance (ANOVA) was conducted, followed by a Bonferroni post-hoc test for pairwise comparisons. Cohen's D test was used to estimate the effect size. Statistical significance was set at $P<0.05$, while $P<0.1$ was considered indicative of a trend.

Results

Animals

The study included horses from nine distinct breeds, along with two horses that were crossbreeds (Table 2). The gender distribution was 64% male (32/50) and 36% female (18/50). The average age of the horses was 6.9 ± 3.7 years, ranging from 3 to 18 years. The results of 46% of the radiographic examinations were categorized as mild osteoarthritis (Table 3). The agreement level among evaluators regarding the osteoarthritis degree was moderate ($\kappa=0.4$; $P<0.001$).

Fractal dimension, bone area fraction, and lacunarity

There was a difference in the BA/TA of the medial ROI among horses with varying OA degrees ($P=0.003$), with lower BA/TA values noted in horses with severe metacarpophalangeal osteoarthritis (Fig. 3). Significant

differences in BA/TA were found between the following OA degrees: absent and mild ($P=0.045$), absent and severe ($P=0.019$), mild and severe ($P<0.001$), and moderate and severe ($P=0.011$). However, no significant differences were detected between male and female horses ($P=0.729$; Table 4).

No statistical differences were found for lateral BA/TA, medial or lateral FD, or medial or lateral lacunarity among animals with varying degrees of OA or between genders ($P>0.1$; Figs. 3–5).

Discussion

In this study, we investigated the radiographic trabecular bone of the proximal phalanx of horses with different degrees of metacarpophalangeal OA, focusing on fractal dimension, lacunarity, and BA/TA. We observed that horses with severe OA exhibited lower BA/TA values in the medial ROI, suggesting a reduced bone density potentially indicative of bone loss associated with the disease's progression. This loss could be linked to the remodeling processes in OA, in which the subchondral plate thickens and becomes sclerotic, but the cancellous bone becomes osteopenic [10]. BA/TA effectively distinguished the most severe OA cases (absent/mild/moderate vs. severe).

Contrary to our hypothesis, horses with milder degrees of metacarpophalangeal OA did not show higher FD and BA/TA values or lower lacunarity in the trabecular bone of the proximal phalanx compared with those with more advanced OA stages. Consequently, this method did not demonstrate sufficient sensitivity for differentiating between the lesser degrees of OA in horses. This finding suggests that the technique may not be ideally suited for analyzing radiographic images in scientific research on this species, particularly for purposes like standardizing study groups or assessing treatment efficacy.

Research indicates that the bone adaptation in the

Table 2. Horse breed distribution from the radiographic examinations used in the study

Breed	Number of animals
American Trotter	30% (15/50)
Brazilian Sport Horse	20% (10/50)
Mangalarga Marchador	16% (8/50)
Quarter Horse	14% (7/50)
Pure Blood Lusitano	6% (3/50)
Thoroughbred	4% (2/50)
Crossbreed	4% (2/50)
Campolina	2% (1/50)
Crioulo	2% (1/50)
Mangalarga	2% (1/50)

Table 3. Classification of radiographic examinations in terms of osteoarthritis (OA) degree

OA degree	Number of examinations
Absent	24% (12/50)
Mild	46% (23/50)
Moderate	22% (11/50)
Severe	8% (4/50)

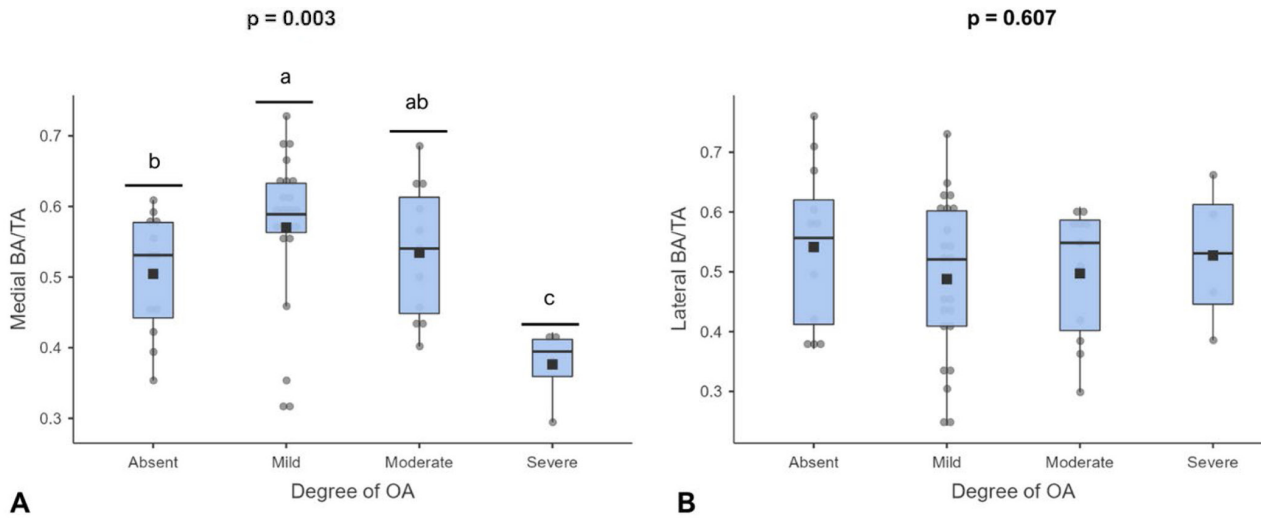


Fig. 3. Box plots of bone area fraction (BA/TA) data from the medial (A) and lateral (B) regions of interest for horses with varying degrees of metacarpophalangeal osteoarthritis (OA). Different lowercase letters indicate statistical differences by Bonferroni post hoc test ($P < 0.05$).

Table 4. Probability (Bonferroni post hoc test) and effect size (Cohen's d) of bone area fraction (BA/TA) values of the medial region of interest as a function of osteoarthritis (OA) degree

OA degree	OA degree	Mean difference	Standard error	t	P	Cohen's d
Absent	- Mild	-0.074	0.036	-2.071	0.045	-0.744
	- Moderate	-0.028	0.048	-0.577	0.567	-0.280
	- Severe	0.156	0.064	2.432	0.019	1.570
Mild	- Moderate	0.046	0.044	1.041	0.304	0.464
	- Severe	0.229	0.061	3.758	<0.001	2.314
Moderate	- Severe	0.183	0.069	2.653	0.011	1.850

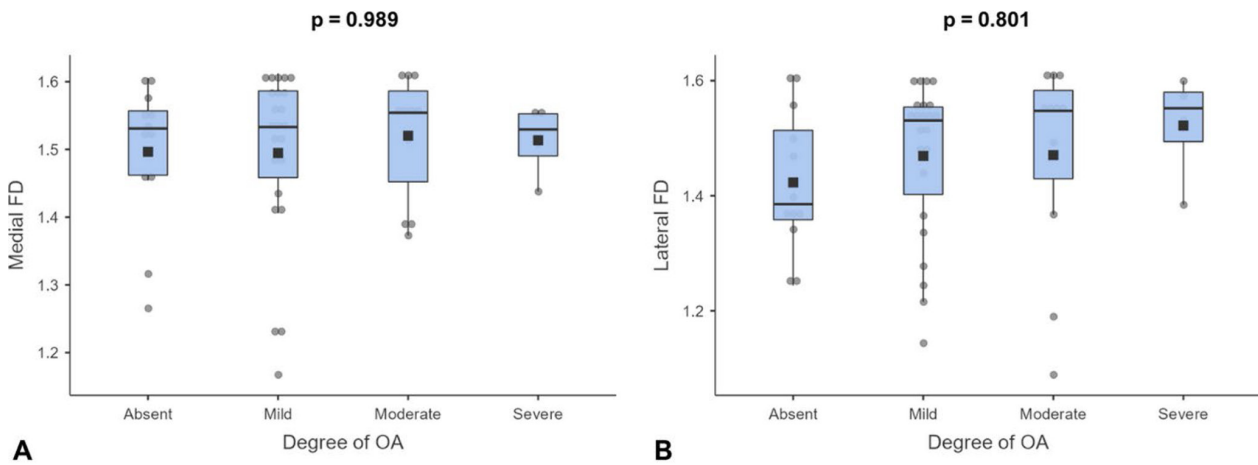


Fig. 4. Box plots illustrating fractal dimension (FD) data from the medial (A) and lateral (B) regions of interest for horses with different degrees of metacarpophalangeal osteoarthritis (OA).

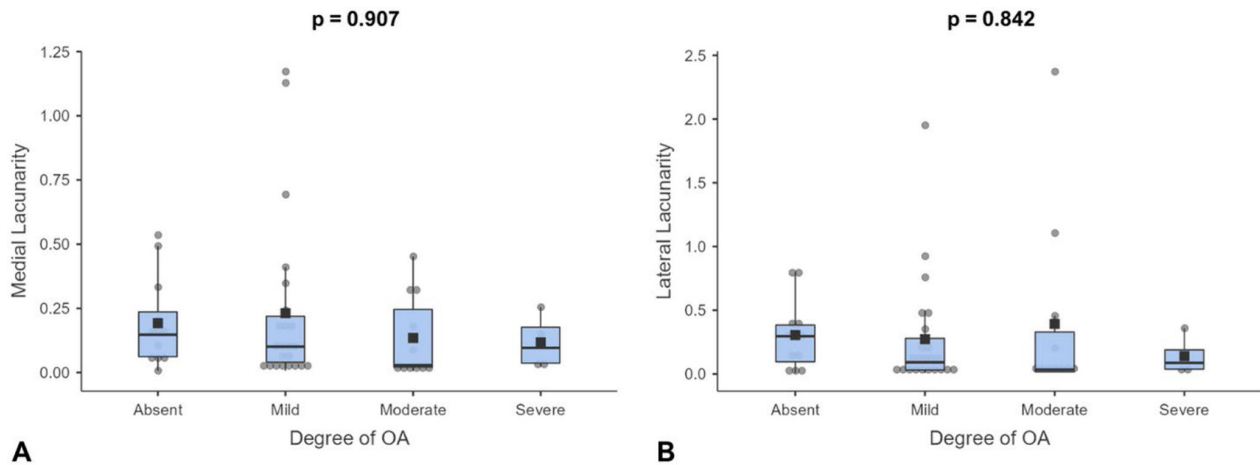


Fig. 5. Box plots illustrating lacunarity data from the medial (A) and lateral (B) regions of interest for horses with different degrees of metacarpophalangeal osteoarthritis (OA).

proximal phalanx is spatially specific, with quadrant-based assessments yielding the most precise insights. Moshage *et al.* (2020) discovered that the medial aspect of the proximal epiphysis of the proximal phalanx in standing horses exhibited a higher strain energy density compared with the lateral aspect, potentially explaining the medial quadrant changes observed in our study [33]. This finding aligns with Harrison *et al.* (2014), who reported greater pressure on the medial contact areas of the metacarpophalangeal joint during horse locomotion [23]. Furthermore, changes in the proximal phalanx, especially pronounced in the medial region, have been reported to be more severe in racing and wild horses [11, 28]. Marsiglia *et al.* (2022) also highlighted the spatial specificity of lesions, noting a predominance of injuries in the medial condyle of the third metacarpal bone [31]. Additionally, the occurrence of injuries on the medial or lateral sides of the limbs has been linked to the type of exercise, with asymmetrical loads impacting the forelimbs [4].

Studies have also shown that humans with osteoarthritis and fractures exhibit lower fractal dimension values in trabecular and cortical bone, while increased lacunarity values of trabecular bone are observed in individuals with osteoporotic changes. These findings suggest that greater bone fragility correlates with decreased complexity and heightened heterogeneity of the bone structure [5, 35, 36]. Nonetheless, our study did not mirror these results.

Among the limitations of this study is the small number of radiographic examinations of the metacarpophalangeal joint categorized as having severe osteoarthritis. The evaluators' agreement on the OA degree was only moderate, reflecting the subjective nature of this method of classification, as it is significantly influenced by each evaluator's clinical experience. Notably, the concordance was higher

for cases classified as severe OA, where bone alterations were more pronounced. This variation in diagnosis could have hampered the ability to derive significant results from the study data.

Additionally, there was considerable variability in the breeds (and thus their functions) and ages of the horses. Cantley *et al.* (1999) highlighted the natural progression of age-related metacarpophalangeal OA in horses and suggested that the stresses of sporting activities could expedite this condition [11]. Sporting activities can be a critical factor in the onset of joint diseases, as they may impose abnormal loads or forces on the joints. Such stresses can induce microdamage to the articular cartilage, which, over time, might lead to metabolic failure of the tissue, characterized by an increase in bone catabolic activity [20].

Our findings suggest that routine radiographic images may not be ideal for evaluating bone changes in horses through fractal analysis and bone area fraction. The technique's sensitivity was insufficient to detect subtle differences in OA degrees, with only severe OA cases being clearly identifiable. This highlights the necessity of accurate classification of bone changes for a proper assessment of cancellous bone, as the two-dimensional nature of radiographic images may not fully capture the nuances of trabecular bone structure, leading to potential information loss.

The use of three-dimensional imaging modalities, such as computed tomography (CT), could offer a more effective means of identifying changes in trabecular bone structure [2, 6]. Future research could benefit from focusing on more homogeneously grouped horses in terms of breed, use, and age and expanding the analysis to other joints. Employing three-dimensional imaging techniques could provide a more detailed and accurate assessment of bone changes.

In summary, fractal dimension, lacunarity, and bone area fraction were not effective in distinguishing differences in the radiographic texture of the trabecular bone in the proximal phalanx among horses with varying degrees of metacarpophalangeal osteoarthritis. Specifically, lower bone area fraction values were noted in the medial side in horses with severe metacarpophalangeal osteoarthritis, suggesting a reduced bone density. However, no significant differences were detected in fractal dimension and lacunarity across different osteoarthritis degrees.

Acknowledgments

This study was supported by the São Paulo Research Foundation (FAPESP; Process No. 2022/14282-7).

References

1. Akaike, H. 1974. A new look at the statistical model identification. *IEEE Trans. Autom.* **19**: 716–723. [[CrossRef](#)]
2. Akkari, H., Bhourri, I., Dubois, P., and Bedoui, M.H. 2008. On the relations between 2D and 3D fractal dimensions: theoretical approach and clinical application in bone imaging. *Math. Model. Nat. Phenom.* **3**: 48–75. [[CrossRef](#)]
3. Aralica, G., Šarec Ivelj, M., Pačić, A., Baković, J., Milković Periša, M., Krištić, A., and Konjevoda, P. 2020. Prognostic Significance of Lacunarity in Preoperative Biopsy of Colorectal Cancer. *Pathol. Oncol. Res.* **26**: 2567–2576. [[Medline](#)] [[CrossRef](#)]
4. Baldwin, C.M., Smith, M.R.W., Allen, S., and Wright, I.M. 2020. Radiographic and arthroscopic features of third carpal bone slab fractures and their impact on racing performance following arthroscopic repair in a population of racing Thoroughbreds in the UK. *Equine Vet. J.* **52**: 213–218. [[Medline](#)] [[CrossRef](#)]
5. Basavarajappa, S., Konddajji Ramachandra, V., and Kumar, S. 2021. Fractal dimension and lacunarity analysis of mandibular bone on digital panoramic radiographs of tobacco users. *J. Dent. Res. Dent. Clin. Dent. Prospect.* **15**: 140–146. [[Medline](#)] [[CrossRef](#)]
6. Alberich-Bayarri, A., Marti-Bonmati, L., Angeles Pérez, M., Sanz-Requena, R., Lerma-Garrido, J.J., García-Martí, G., and Moratal, D. 2010. Assessment of 2D and 3D fractal dimension measurements of trabecular bone from high-spatial resolution magnetic resonance images at 3 T. *Med. Phys.* **37**: 4930–4937. [[Medline](#)] [[CrossRef](#)]
7. Bollen, A.M., Taguchi, A., Hujoel, P.P., and Hollender, L.G. 2001. Fractal dimension on dental radiographs. *Dentomaxillofac. Radiol.* **30**: 270–275. [[Medline](#)] [[CrossRef](#)]
8. Borys, P., Krasowska, M., Grzywna, Z.J., Djamgoz, M.B.A., and Mycielska, M.E. 2008. Lacunarity as a novel measure of cancer cells behavior. *Biosystems* **94**: 276–281. [[Medline](#)] [[CrossRef](#)]
9. Britt, L.G., and Tucker, R.L. 2010. Articulação metacarpofalangeana/ metatarsofalangeana. pp. 917–944. *In: Diagnóstico de Radiologia Veterinária*, 5th ed. (Thrall, D.E. ed.), Elsevier, Rio de Janeiro.
10. Burr, D.B., and Gallant, M.A. 2012. Bone remodelling in osteoarthritis. *Nat. Rev. Rheumatol.* **8**: 665–673. [[Medline](#)] [[CrossRef](#)]
11. Cantley, C.E.L., Firth, E.C., Delahunty, J.W., Pfeiffer, D.U., and Thompson, K.G. 1999. Naturally occurring osteoarthritis in the metacarpophalangeal joints of wild horses. *Equine Vet. J.* **31**: 73–81. [[Medline](#)] [[CrossRef](#)]
12. Cesur, E., Bayrak, S., Kursun-Çakmak, E.S., Arslan, C., Köklü, A., and Orhan, K. 2020. Evaluating the effects of functional orthodontic treatment on mandibular osseous structure using fractal dimension analysis of dental panoramic radiographs. *Angle Orthod.* **90**: 783–793. [[Medline](#)] [[CrossRef](#)]
13. Chen, Q., Bao, N., Yao, Q., and Li, Z.Y. 2018. Fractal dimension: a complementary diagnostic indicator of osteoporosis to bone mineral density. *Med. Hypotheses* **116**: 136–138. [[Medline](#)] [[CrossRef](#)]
14. Chirchir, H., Ruff, C.B., Junno, J.A., and Potts, R. 2017. Low trabecular bone density in recent sedentary modern humans. *Am. J. Phys. Anthropol.* **162**: 550–560. [[Medline](#)] [[CrossRef](#)]
15. Cordeiro, M.S., Backes, A.R., Júnior, A.F.D., Gonçalves, E.H.G., and de Oliveira, J.X. 2016. Fibrous dysplasia characterization using lacunarity analysis. *J. Digit. Imaging* **29**: 134–140. [[Medline](#)] [[CrossRef](#)]
16. Cui, J., Liu, C.L., Jennane, R., Ai, S., Dai, K., and Tsai, T.Y. 2023. A highly generalized classifier for osteoporosis radiography based on multiscale fractal, lacunarity, and entropy distributions. *Front. Bioeng. Biotechnol.* **11**: 1054991. [[Medline](#)] [[CrossRef](#)]
17. Doube, M., Kłosowski, M.M., Arganda-Carreras, I., Cordelières, F.P., Dougherty, R.P., Jackson, J.S., Schmid, B., Hutchinson, J.R., and Shefelbine, S.J. 2010. BoneJ: free and extensible bone image analysis in ImageJ. *Bone* **47**: 1076–1079. [[Medline](#)] [[CrossRef](#)]
18. Fazzalari, N.L., and Parkinson, I.H. 1996. Fractal dimension and architecture of trabecular bone. *J. Pathol.* **178**: 100–105. [[Medline](#)] [[CrossRef](#)]
19. Fazzalari, N.L., and Parkinson, I.H. 1997. Fractal properties of subchondral cancellous bone in severe osteoarthritis of the hip. *J. Bone Miner. Res.* **12**: 632–640. [[Medline](#)] [[CrossRef](#)]
20. Frisbie, D.D., and Johnson, S.A. 2019. Synovial Joint Biology and Pathobiology. pp. 200–225. *In: Equine Surgery*, 5th ed. (Auer, J.A., Stick, J.A., Kümmerle, J.M., Orange, T. eds.), Elsevier, Missouri.
21. Gallucci, M. 2019. GAMLj: General Analysis for the Linear Model in Jamovi.
22. Geraets, W.G.M., and van der Stelt, P.F. 2000. Fractal properties of bone. *Dentomaxillofac. Radiol.* **29**: 144–153. [[Medline](#)] [[CrossRef](#)]

23. Harrison, S.M., Whitton, R.C., Kawcak, C.E., Stover, S.M., and Pandey, M.G. 2014. Evaluation of a subject-specific finite-element model of the equine metacarpophalangeal joint under physiological load. *J. Biomech.* **47**: 65–73. [[Medline](#)] [[CrossRef](#)]
24. He, T., Cao, C., Xu, Z., Li, G., Cao, H., Liu, X., Zhang, C., and Dong, Y. 2017. A comparison of micro-CT and histomorphometry for evaluation of osseointegration of PEO-coated titanium implants in a rat model. *Sci. Rep.* **7**: 16270. [[Medline](#)] [[CrossRef](#)]
25. Jolley, L., Majumdar, S., and Kapila, S. 2006. Technical factors in fractal analysis of periapical radiographs. *Dentomaxillofac. Radiol.* **35**: 393–397. [[Medline](#)] [[CrossRef](#)]
26. Karadag, I., and Yilmaz, H.G. 2022. Evaluation of change in trabecular bone structure surrounding dental implants by fractal dimension analysis and comparison with radiomorphometric indicators: a retrospective study. *PeerJ* **10**: e13145. [[Medline](#)] [[CrossRef](#)]
27. Kato, C.N.A.O., Barra, S.G., Tavares, N.P.K., Amaral, T.M.P., Brasileiro, C.B., Mesquita, R.A., and Abreu, L.G. 2020. Use of fractal analysis in dental images: a systematic review. *Dentomaxillofac. Radiol.* **49**: 20180457. [[Medline](#)] [[CrossRef](#)]
28. Kawcak, C.E., and McIlwraith, C.W. 1994. Proximodorsal first phalanx osteochondral chip fragmentation in 336 horses. *Equine Vet. J.* **26**: 392–396. [[Medline](#)] [[CrossRef](#)]
29. Lacitignola, L., Imperante, A., Staffieri, F., De Siena, R., De Luca, P., Muci, A., and Crovace, A. 2020. Assessment of Intra-and inter-observer measurement variability in a radiographic metacarpophalangeal joint osteophytosis scoring system for the horse. *Vet. Sci.* **7**: 39. [[Medline](#)] [[CrossRef](#)]
30. Maquer, G., Musy, S.N., Wandel, J., Gross, T., and Zysset, P.K. 2015. Bone volume fraction and fabric anisotropy are better determinants of trabecular bone stiffness than other morphological variables. *J. Bone Miner. Res.* **30**: 1000–1008. [[Medline](#)] [[CrossRef](#)]
31. Marsiglia, M.F., Yamada, A.L.M., Agreste, F.R., de Sá, L.R.M., Nieman, R.T., and da Silva, L.C.L.C. 2022. Morphological analysis of third metacarpus cartilage and subchondral bone in Thoroughbred racehorses: an ex vivo study. *Anat. Rec. (Hoboken)* **305**: 3385–3397. [[Medline](#)] [[CrossRef](#)]
32. Mishra, S., Kumar, M., Mishra, L., Mohanty, R., Nayak, R., Das, A.C., Mishra, S., Panda, S., and Lapinska, B. 2022. Fractal dimension as a tool for assessment of dental implant stability—a scoping review. *J. Clin. Med.* **11**: 4051. [[Medline](#)] [[CrossRef](#)]
33. Moshage, S.G., McCoy, A.M., Polk, J.D., and Kersh, M.E. 2020. Temporal and spatial changes in bone accrual, density, and strain energy density in growing foals. *J. Mech. Behav. Biomed. Mater.* **103**: 103568. [[Medline](#)] [[CrossRef](#)]
34. Palanivel, D.A., Natarajan, S., Gopalakrishnan, S., and Jennane, R. 2020. Multifractal-based lacunarity analysis of trabecular bone in radiography. *Comput. Biol. Med.* **116**: 103559. [[Medline](#)] [[CrossRef](#)]
35. Podsiadlo, P., Dahl, L., Englund, M., Lohmander, L.S., and Stachowiak, G.W. 2008. Differences in trabecular bone texture between knees with and without radiographic osteoarthritis detected by fractal methods. *Osteoarthritis Cartilage* **16**: 323–329. [[Medline](#)] [[CrossRef](#)]
36. Rabelo, G.D., Roux, J.P., Portero-Muzy, N., Gineyts, E., Chapurlat, R., and Chavassieux, P. 2018. Cortical fractal analysis and collagen crosslinks content in femoral neck after osteoporotic fracture in postmenopausal women: comparison with osteoarthritis. *Calcif. Tissue Int.* **102**: 644–650. [[Medline](#)] [[CrossRef](#)]
37. Sánchez, I., and Uzcátegui, G. 2011. Fractals in dentistry. *J. Dent.* **39**: 273–292. [[Medline](#)] [[CrossRef](#)]
38. de Souza Santos, D., Dos Santos, L.C., de Albuquerque Tavares Carvalho, A., Leão, J.C., Delrieux, C., Stosic, T., and Stosic, B. 2016. Multifractal spectrum and lacunarity as measures of complexity of osseointegration. *Clin. Oral Investig.* **20**: 1271–1278. [[Medline](#)] [[CrossRef](#)]
39. Saers, J.P.P., DeMars, L.J., Stephens, N.B., Jashashvili, T., Carlson, K.J., Gordon, A.D., Ryan, T.M., and Stock, J.T. 2021. Automated resolution independent method for comparing in vivo and dry trabecular bone. *Am. J. Phys. Anthropol.* **174**: 822–831. [[Medline](#)] [[CrossRef](#)]
40. Silva, M.M., Hagen, S.C.F., Vendruscolo, C.P., Baccarin, R.Y.A., Spagnolo, J.D., Yamada, A.L.M., Stievani, F.C., and Silva, L.C.L.C. 2019. The correlation between score-based protocol for equine joint assessment and subsequent arthroscopic intervention outcomes. *Braz. J. Vet. Res. Anim. Sci.* **56**: e158072. [[CrossRef](#)]
41. Southard, T.E., Southard, K.A., Jakobsen, J.R., Hillis, S.L., and Najim, C.A. 1996. Fractal dimension in radiographic analysis of alveolar process bone. *Oral Surg. Oral Med. Oral Pathol. Oral Radiol. Endod.* **82**: 569–576. [[Medline](#)] [[CrossRef](#)]
42. The jamovi project, 2021. Jamovi.
43. Yaşar, F., and Akgünlü, F. 2005. Fractal dimension and lacunarity analysis of dental radiographs. *Dentomaxillofac. Radiol.* **34**: 261–267. [[Medline](#)] [[CrossRef](#)]
44. Zandieh, S., Haller, J., Bernt, R., Hergan, K., and Rath, E. 2017. Fractal analysis of subchondral bone changes of the hand in rheumatoid arthritis. *Medicine (Baltimore)* **96**: e6344. [[Medline](#)] [[CrossRef](#)]